

Article

# Apparatus for Scalable Functionalization of Single-Walled Carbon Nanotubes via the Billups-Birch Reduction

David Pham <sup>1</sup>, Kevin S. Zhang <sup>1</sup>, Olawale Lawal <sup>1</sup>, Saunab Ghosh <sup>1,2</sup>, Varun Shenoy Gangoli <sup>1,2</sup>, Thomas J. Ainscough <sup>3</sup>, Bernie Kellogg <sup>1</sup>, Robert H. Hauge <sup>1,†</sup>, W. Wade Adams <sup>1,2,4</sup> and Andrew R. Barron <sup>2,3,4,\*</sup>

<sup>1</sup> Smalley-Curl nanoCarbon Center, Rice University, Houston, TX 77005, USA; dtp4@rice.edu (D.P.); ksz3@rice.edu (K.S.Z.); wale.b.lawal@gmail.com (O.L.); saunab@rice.edu (S.G.); varunshenoyg@rice.edu (V.S.G.); bernie.kellogg@rice.edu (B.K.); wadams@rice.edu (W.W.A.)

<sup>2</sup> Department of Chemistry, Rice University, Houston, TX 77005, USA

<sup>3</sup> Energy Safety Research Institute, Swansea University Bay Campus, Swansea SA1 8EN, UK; 526025@swansea.ac.uk

<sup>4</sup> Department of Materials Science and Nanoengineering, Rice University, Houston, TX 77005, USA

\* Correspondence: arb@rice.edu or a.r.barron@swansea.ac.uk; Tel.: +1-713-348-5610

† Died 17 March 2016.

Received: 25 May 2017; Accepted: 14 June 2017; Published: 17 June 2017

**Abstract:** A prototype design of a reactor for scalable functionalization of SWCNTs by the reaction of alkyl halides with Billups-Birch reduced SWCNTs is described. The Hauge apparatus is designed to allow for the safe handling of all the reagents and products under an inert atmosphere at controlled temperatures. The extent of reaction of Li/NH<sub>3</sub> solution with the SWCNTs is measured in-situ by solution conduction, while homogenous mixing is ensured by the use of a homogenizer, and thermocouple are placed at different heights within the reactor flask. Addition of an alkyl halide yield alkyl-functionalized SWCNTs, which may be isolated by solvent extraction leaving a solid sample that is readily purified by hydrocarbon extraction. As an example, reaction of SWCNT/Li/NH<sub>3</sub> with 1-iododecane yields dodecane-functionalized SWCNTs (C<sub>12</sub>-SWCNTs), which have been characterized by TG/DTA, XPS, and Raman spectroscopy. Sample extraction during the reaction allows for probing of the rate of the reaction in order to determine the end point of the reaction, which for C<sub>12</sub>-SWCNTs (at −78 °C) is 30 min.

**Keywords:** carbon nanotube; lithium; reduction; functionalization; ammonia

## 1. Introduction

An unfortunate side effect of the all-carbon structure of single walled carbon nanotubes (SWCNTs) is they are highly hydrophobic in nature, which results in insolubility in common solvents and immiscibility in many polymeric materials. Both of which limits the ability to process them for many applications [1]. Thus, an ongoing area of interest is the formation of individual SWCNTs rather than bundles or aggregates. Several methods have been used to functionalize SWCNT bundles with solubilizing substituents; however, only some methods exfoliate the bundles. Solubilization (miscibility) is made possible through either wrapping (surfacting) the SWNTs [2], end-group functionalization [3,4], or sidewall functionalization [5,6]. Of these, it is the latter that has generated the most interest because of the wide range of functional groups it is possible to employ and the diverse methods for functionalization, including: free radical additions [7], reactions with acids [8], aryldiazonium salts [9], carbenes and nitrenes [10]. Furthermore, fluorination of the sidewalls leads to tubes that may be further functionalized by organolithium or Grignard reagents or primary amines [11,12] as well

as Diels–Alder (4 + 2) cycloaddition reaction [13]. The majority of these approaches have only been carried out on a small scale; however, as SWCNTs become more economically viable, developing large scalable process for their functionalization becomes increasingly important.

One non-destructive approach that we believe has potential for large scale production of functionalized SWCNTs is the reaction of alkyl halides with reduced SWCNTs formed upon the reaction of SWCNTs with Group 1 metals [14–16]. Using the Wilds and Nelson modification (Li metal in liquid  $\text{NH}_3$ ) of the Birch reduction (Na metal in liquid  $\text{NH}_3$ ) [17,18], Billups and co-workers reported that SWCNTs were reduced to form solubilized anions that react with alkyl halides via a alkyl radical intermediates [14]. Nanotubes that are highly soluble in solvents such as chloroform, THF and water may be prepared depending on the choice of substituent.

The advantage of the Billups-Birch route is that a wide range of substituents may be employed [19,20]. For the effective functionalization of SWCNTS, a typical Billups–Birch reaction process is performed in a three-neck flask/Dewar condenser setup for 24 h with the flask submerged in an acetone-dry ice mixture. However, this generic simple setup has several limitations, as we don't get actual information on the reaction kinetics and the duration of reaction. The scalable synthesis of highly solubilized undamaged nanotubes requires more robust and controllable approach. In this report, we introduce a state-of-the-art apparatus to functionalize SWCNTS in highly reproducible manner.

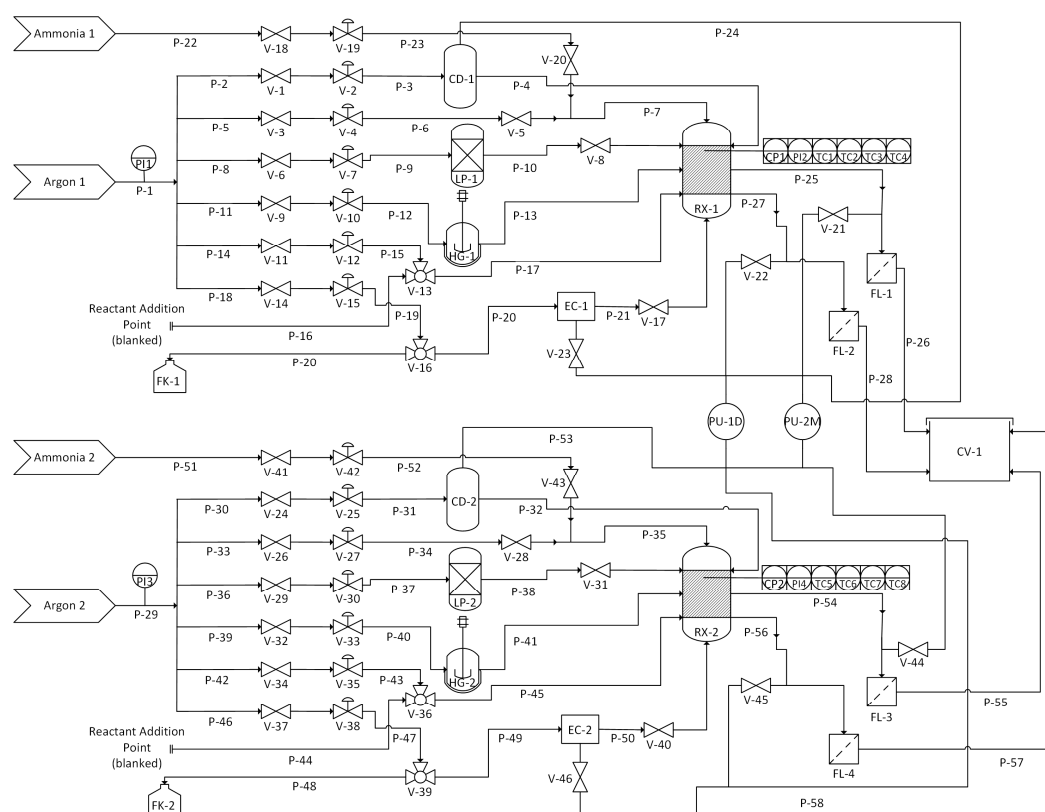
The use of  $\text{Li}/\text{NH}_3$  at commercial scale is has been investigated previously, and much can be learnt from these efforts. In particular, Joshi et al., have discussed the issues with running a  $\text{Li}/\text{NH}_3$  reduction reaction, at production plant levels, as part of the synthesis of a drug candidate: Sumanrole Maleate [21], in particular challenges relating to the design of the equipment, choice and handling of materials, operations, and waste treatment. We have approached the creation of a flexible, safe and controllable process through the design of a reactor apparatus that can be reproduced in other laboratories. Herein we report an apparatus, designed by our late colleague and collaborator Robert Hauge that allows for not only scalability in running simultaneous samples and re-cycling the  $\text{NH}_3$  solvent (an important concern for commercialization), but provides in-situ monitoring and sample extraction. We have named the system in his memory.

## 2. Results and Discussion

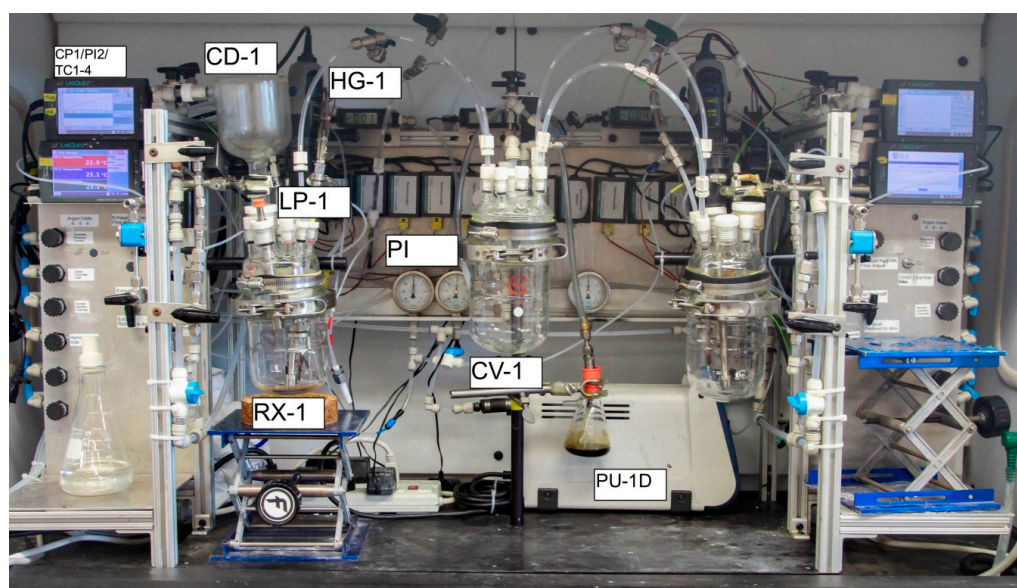
### 2.1. Apparatus Design and Operation

Figure 1 shows a schematic representation of the Hauge apparatus, while Figure 2 shows a photograph of the twin reactor system. This new apparatus allows large-scale (300–500 mg) functionalization of SWCNTs in a single step. The major components of this advanced apparatus include two customized multiple-neck reaction flasks (RX-1 and RX-2) (for two simultaneous reactions) each attached to Dewar condenser (CD) and a sample extraction chamber (EC). Reaction flasks are connected to a mechanical pump (PU) and multiple inert gas supply lines. In order to monitor temperature and conductivity of the reactants, pressure and gas flow inside the flasks, this apparatus is equipped with various electronic probes attached to digital data collection devices (see Figures 1 and 2). Thus, the setup allows for the monitoring and recording of important reaction parameters, such as conductivity and temperature of the  $\text{Li}/\text{NH}_3$  solution during reaction process.

Prior to functionalization of SWCNTs the apparatus was checked for leaks to ensure that no adventitious oxidation (of the reduced species) occurs. The apparatus was evacuated for 10 min by a mechanical pump (PU) to a pressure of ~20 Torr. After closing the pump inlet valve (V-21/V-44) the pressure inside a reaction flask was continuously recorded for 20 min by an electronic pressure gauge attached to a LabQuest 2 digital data collection device (Vernier, CP/TC connections). As shown by Figure 3, only a small pressure change (40 Torr) was observed after an interval of 20 min due small gaps inside the homogenizer shaft. The test confirmed that this apparatus was almost free of leaks and ideal for running reactions in inert environment.



**Figure 1.** Schematic representation of the dual reactor apparatus: P—pipe, V—valve, PI—pressure indicator, CD—condenser, LP—lithium purge, HG—homogenizer, FK—round bottom flask, FL—filter, RX—reactor, EC—extraction chamber, CP—conductivity probe, TC—thermocouple, CV—collection vessel, PU-1D—diaphragm pump, PU-2M—mechanical pump.



**Figure 2.** Photograph of the Hauge twin reactor system: PI—pressure indicator, CD-1—condenser, LP-1—lithium purge, HG-1—homogenizer, RX-1—reactor, CP-1—conductivity probe, TC-1-4—thermocouple, CV-1—collection vessel, PU-1D—diaphragm pump.

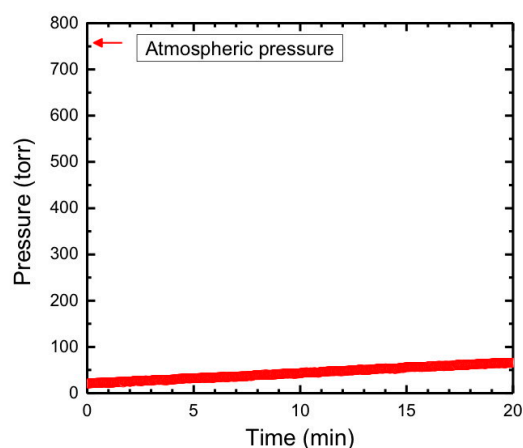


**Figure 3.** Pressure inside reaction flask as a function of time after evacuation.

## 2.2. Hazards Associated with Lithium Metal and Ammonia

One of the main goals in the design described above is to provide a safe process; however, due to the hazards associated with the handling of Li metal and liquid  $\text{NH}_3$  it is worth reviewing risks and appropriate protocols.

Metallic Li reacts violently with water to give off flammable explosive  $\text{H}_2$ . The reaction with air,  $\text{N}_2$ , and  $\text{NH}_3$  result in the formation of the oxide ( $\text{Li}_2\text{O}$ ), nitride ( $\text{Li}_3\text{N}$ ), and amide ( $\text{LiNH}_2$ ), respectively. Once a container of Li is opened, unused metal should be stored in mineral oil or under argon. Solid Li metal will cause skin and eye burns, as it reacts with moisture to form corrosive hydroxide ( $\text{LiOH}$ ). When fighting Li fires, use of dry graphite powder or dry LiCl is recommended. Most importantly, water, sand,  $\text{CO}_2$ , dry chemical, or halon should not be used.

Ammonia is highly corrosive and irritating to the skin, eyes, and respiratory system. The boiling point of liquid ammonia is  $-33\text{ }^\circ\text{C}$ , and so the temperature of all reactions should be monitored carefully. The use of dry ice-acetone bath ( $-78\text{ }^\circ\text{C}$ ) ensures sufficient cooling at all times and the presence of multiple thermocouples being placed at different points in the reactor to ensure that localized heating is not occurring. If the temperature does increase during the reaction there is the risk of over pressurization in the vessel. Thus, the pressure is monitored and a controllable exhaust line allows pressure to be relieved from the flask via a safety valve. It is essential to eliminate all leaks, provide good ventilation, and install suitable  $\text{NH}_3$  alarms near the equipment.

## 2.3. Example of SWCNT Functionalization

In order to demonstrate the suitability of the Hauge apparatus we have performed a typical alkylation reaction that can be compared to previous results [14,22]. Reaction with 1-iododecane yield dodecane-functionalized SWCNTs ( $\text{C}_{12}$ -SWCNTs), whose solubility allows for ease of characterization. A sample of  $\text{C}_{12}$ -SWCNTs was prepared (see Experimental) and characterized by thermal gravimetric analysis (TGA) and Raman spectroscopy in comparison with the literature reported derivative [22].

A TGA on a dodecylated sample ( $\text{C}_{12}$ -SWCNTs) was performed to determine the extent of functionalization and to correlate weight loss data with the carbon/alkyl group ratio. Using continuous heating of a  $\text{C}_{12}$ -SWCNTs sample under an argon atmosphere from  $25\text{ }^\circ\text{C}$  to  $700\text{ }^\circ\text{C}$ , a mass loss of 40.6% was observed (Figure 4a). After accounting for the 21% residual iron catalyst content in our sample (from Figure 4b), we calculate that the mass loss during pyrolysis implied an initial composition of one  $\text{C}_{12}\text{H}_{25}$  group per 16.3 SWCNT carbon atoms. This ratio is consistent with, but slightly higher than, the ratio (one  $\text{C}_{12}\text{H}_{25}$  group per 24 SWCNT carbon atoms) reported by Liang et al., for similar dodecylated samples [22].

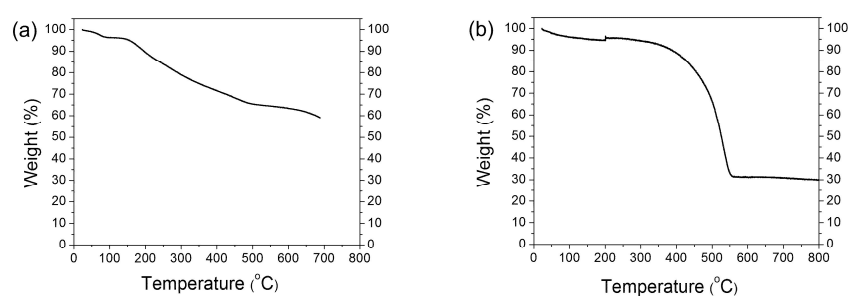


**Figure 4.** TGA of (a) C<sub>12</sub>-SWCNTs measured under Ar atmosphere and (b) chlorine purified HiPco SWNTs measured under air.

Figure 5 compares the Raman spectra of the chlorine purified HiPco SWCNTs and C<sub>12</sub>H<sub>25</sub> functionalized HiPco SWCNTs. The tangential mode (G band) of the SWCNTs appears as a strong peak at ca. 1590 cm<sup>-1</sup> with a shoulder at ca. 1560 cm<sup>-1</sup>, and the disorder mode (D band) centered at ca. 1350 cm<sup>-1</sup>. The ratio of the intensities of D and G band peaks (D:G ratio) provides a qualitative analysis of the extent of functionalization. Generally, the higher the D:G ratio, the higher the extent to which the SWCNTs have been functionalized; however, we note that variations also occur for changes in the special distribution of functional groups [23]. However, the comparison is valid for different samples of the same functional group prepared by similar procedures. The precursor nanotubes have a near zero D:G ratio as a result of no functionalization, whereas the C<sub>12</sub>H<sub>25</sub> functionalized sample shown in Figure 5b has a D:G ratio of 0.955. This particular sample was functionalized for 30 min, and it exceeds reported values in literature for the same reaction conditions in previous iterations of a Birch reduction apparatus [22]. Based on the implementation of identical reaction conditions using the same functionalization chemistry as reported previously [14,22], we propose the functional groups are strongly attached to the SWCNT walls with a minimal increase in the average SWCNT diameter post-functionalization.

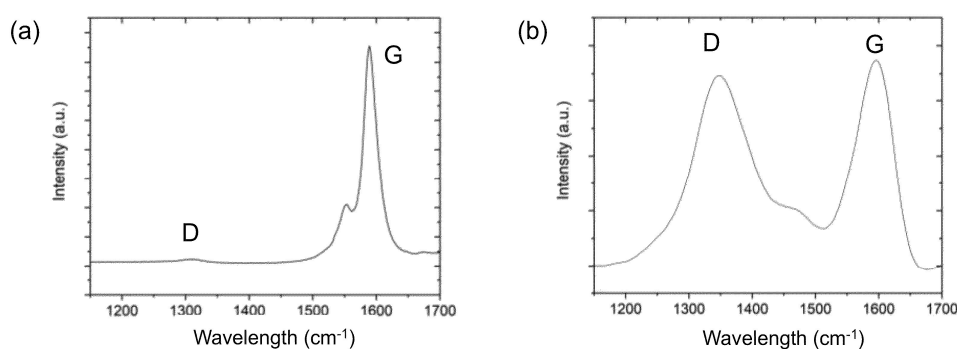


**Figure 5.** Raman spectrum (514 nm) of (a) chlorine-purified HiPco SWNTs and (b) C<sub>12</sub>-SWCNTs.

The TGA and Raman data are therefore consistent with a slight improvement in the efficiency of functionalization using the present system. Based upon the forgoing it is clear that this system allows for the successful synthesis of alkyl-functionalized SWCNTs.

#### 2.4. Monitoring the Alkylation Reaction

As reported in the original literature [14,22] the liquid NH<sub>3</sub> was evaporated after the addition of the functional group (alkyl halide). It was assumed that this provided sufficient time for the reaction to reach completion. The reactor described herein offers the advantage that aliquots of the reaction mixture may be taken at any time. This capability further helps understanding of the reaction progress,

which in turn provides important information, such as the effect of catalyst residue and extent of functionalization with time, in order to determine the most efficient, scalable method/protocol of functionalizing nanotubes.

In the present case aliquots were taken in-situ to track the progress of the reaction. These results were compared with those after 24 h reaction. The Raman spectra were obtained for each sample (Figure 6 shows the spectra for the samples with reaction time  $1 \leq t \leq 20$  min). Although the D:G ratio is often assumed to be a direct measure of functionalization [24], it is also dependent on the distribution of functional groups [23], making it hard to directly compare different sample types. However, in the present case where the functionalization is occurring in a single system, changes in special distribution should not be significant, and thus the D:G ratio is a good indicator of the extent of reaction.

By comparing the D:G ratios for each sample the progress of the reaction can be tracked and as may be seen from Figure 7, 30 min appears to be an adequate time for the functionalization of SWCNTs to complete since the results are essentially indistinguishable from a sample prepared with 24 h reaction time. It should be noted that we use a condenser with a dry ice/acetone bath to prevent loss of  $\text{NH}_3$  from evaporation before the 30 min. reaction time is done.

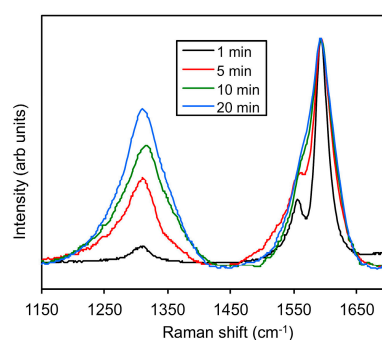


**Figure 6.** Raman spectra (633 nm) of the products from the reaction of Billups-Birch reduced HiPco SWCNTs and 1-iododecane as a function of reaction time ( $1 \leq t \leq 20$  min). The spectra are normalized to the G peak for ease of comparison.

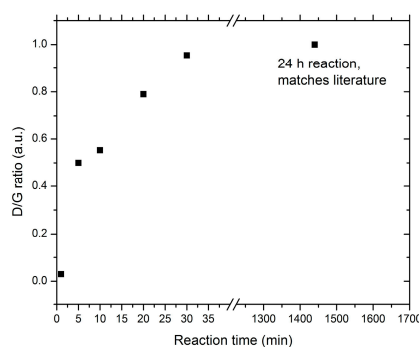


**Figure 7.** Plot of D:G ratio from the Raman spectra of the products from the reaction of Billups-Birch reduced HiPco SWCNTs and 1-iododecane as a function of reaction time. The 30-min sample has a D:G ratio that matches reported literature values from reactions for 24 h.

### 3. Experimental Section

#### 3.1. Materials and Characterization

Pristine HiPco single-walled carbon nanotubes (SWCNTs), 09-HiPco-0093 batch No. 190.1, were obtained from the Carbon Nanotube Laboratory (CNL) at Rice University and used as received.

Lithium (granule, high sodium, 99%), tetrahydrofuran ( $\geq 99.9\%$ ), hexane ( $\geq 98.5\%$  concentration), 1-iododecane (98% concentration), acetone, ethanol (200 proof), and Millipore PTFE (0.2  $\mu\text{m}$ ) filter paper were obtained from Sigma-Aldrich (St. Louis, MO, USA) and used as received unless otherwise noted. All tubing used for the reactor was Teflon<sup>TM</sup> obtained from Cole-Palmer or United States Plastic Corp (Shanghai, China). Chlorine treatment of SWCNTs was adapted from the literature [25].

Thermogravimetric analysis (TGA) was performed on a Seiko TG/DTA 200. The iron percentage and extent of functionalization was measured using ca. 10 mg of sample placed in a platinum pan and heated under ambient conditions up to 800 °C in dry air with a ramp rate was 5 °C  $\text{min}^{-1}$ , and sampling interval of 3 s. Raman was carried out on a Renishaw inVia Raman Microscope using three laser lines for characterization; these were 514 nm (2.41 eV), 633 nm (1.96 eV), and 785 nm (1.58 eV). To maximize the Raman signal a continuous scan was carried out of the G peak ( $\sim 1600 \text{ cm}^{-1}$ ), while the focus of the beam was altered to maximize the G peak intensity. When the maximal intensity was found, data was acquired using an integration of 10 accumulations at a power of 10%, with cosmic ray background removal applied. Each sample was probed a number of times at a variety of locations, to acquire data that represented the entirety of the sample. Raman data was acquired for a range of wavenumbers ranging from 100–3300  $\text{cm}^{-1}$ .

### 3.2. Apparatus

A schematic representation of the apparatus is shown in Figure 1, while a photograph of the actual apparatus is provided in Figure 2. Argon flow originates from a tank and enters reaction flask, RX, through homogenizer, HG, general chamber, CD, or an external tube, LP, for degassing lithium before insertion into the reactor flask, RX. Flowmeters on each side display Ar flow, allowing controlled flow of inert gas during reaction. An adjustable inlet with pressure control manages  $\text{NH}_3$  gas flow into the system (V-19, V-42). Prior to reaction SWCNT samples are dried in vacuum using a mechanical pump, PU-2M. The diaphragm pump, PU-1D, allows transfer of large amounts of liquids and gases to a collection flask, CV-1, or small aliquots of solids to an extraction line, EC. Each reactor has a line to the middle flask with a detachable Swagelok filter, FL. Filters pores range from 15–40  $\mu\text{m}$ . Liquid solvents can be extracted to the sample collector (CV), leaving solid sample behind in the reactor. A CAT  $\times 120$  homogenizer (HG-1, HG-2) with shear mixing serves as the dissolution mechanism for improved homogenous mixing relative to a standard stir bar. A LabQuest Pro conductivity probe (Vernier, LP-1 and LP-2) measures conductivity in-situ. Probe tips were changed to titanium electrodes. The probe determines conductivity by measuring current when a potential difference is applied. A 2 point calibration is performed with Nanopure 18 M $\Omega$  water and LabQuest standard 500 mg/L (1000  $\mu\text{S}/\text{cm}$ ) NaCl solution in Nanopure water. Three K-type (Ni-Cr/Ni-Al) thermocouple wires (TC-1–TC-8) are placed at different heights within a reactor flask to read temperatures in-situ at varying levels in the reactor. Reaction temperatures are displayed using a Vernier Labquest Pro digital display. Mechanical and electronic pressure sensors maintain control of the flask environment. A controllable exhaust line allows pressure to be relieved from the flask. A safety valve automatically releases gases if the pressure is too high. Lithium is held in a  $\frac{1}{4}$ " glass tube outside of the reactor and purged with argon for 1 min prior to insertion. A needle valve allows passage of lithium into reactor from insertion chamber after purging. Aliquots can be taken to monitor reaction kinetics. A combination of positive pressure and vacuum extract the sample from a narrow hole to the collection filter membrane.

### 3.3. Alkylation of SWCNTs

Functionalization proceeds according to methods described by Billups' alkylation of nanotubes using Birch reduction [14,22]. In a typical reaction, SWCNTs (50 mg) were added to the 700 mL reaction flask and heated under vacuum at 180 °C for 10 min. in order to remove adsorbed gases. Argon gas continuously flows through the system to create an inert atmosphere. The flask is submerged in the dry ice-acetone bath to condense  $\text{NH}_3$  (300 mL). Li metal was added in molar quantities (C:Li = 1:1–1:3), via the lithium purge (LP-1/LP-2), until a conductive solution is created as measured by the conductivity

probes (CP1/CP2). The shear-mixing homogenizer (HG1/HG2) ensures homogeneity of the solution. 1 h after the Li addition, 1-iododecane (4 mL) was added using a syringe via lithium purge inlet along with THF solvent (6 mL) to prevent reactant from solidifying under reaction conditions. Aliquots were taken to monitor reaction kinetics via extraction chamber (EC-1/EC-2). The sample collects for approximately 1 min per aliquot sample. The solution is stirred for 2 h, after which the liquid NH<sub>3</sub> is extracted to the sample collector (CV-1) to prevent contamination of the functionalized product from any side products formed during reaction. C<sub>12</sub>-SWCNTs are extracted into a separatory funnel, separate from the reactor. To this was added ethanol (150 mL), DI water (150 mL), and hexane (200 mL). A solution of diluted HCl (10 mL) was added to the funnel and the solution is vigorously shaken. The hexane layer is filtered through a cellulose filter paper after separation from the water/ethanol layer. Products are vacuum-dried overnight.

#### 4. Conclusions

We have reported a flexible apparatus for the scalable alkylation of SWCNTs using the Billups-Birch reduction process in liquid NH<sub>3</sub>. The advantages of our new apparatus include: the solid reactants are treated in an inert atmosphere to prohibit unwanted oxygen inclusion, the liquid reactants are automatically added to the reaction flask by a controlled injection system, and the intermediate partially functionalized products can be systematically extracted to monitor the reaction. The conductivity versus time profile indicates that a typical alkylation reaction of SWCNTs ends much earlier (within 30 min) and requires less metallic lithium than earlier reported [14,22]. The cost-efficient features of this apparatus: at the end of a reaction cycle the excess NH<sub>3</sub> can be separated and transferred to the second reaction flask reutilized for another functionalization reaction cycle. The reproducibility of reaction process further confirms that this apparatus is ideal for bulk functionalization of SWCNTs.

**Acknowledgments:** This work was supported by the Office of Naval Research (N00014-15-2717), the Welsh Government Sêr Cymru National Research Network in Advanced Engineering and Materials (NRN-150), the Robert A. Welch Foundation (C-0002), and Lockheed Martin Corporation. We also acknowledge Steve Ripley's help in the construction of the apparatus.

**Author Contributions:** David Pham and Kevin S. Zhang were involved in the design, construction and testing of the apparatus; Olawale Lawal helped build the apparatus, performed experiments and characterization; Saunab Ghosh built and leak checked the apparatus, and performed functionalization experiments and characterization; Varun Shenoy Gangoli helped leak check the apparatus and contributed to discussions of the experiments and results; Thomas J. Ainscough created the P&ID for the apparatus; Bernie Kellogg was involved in discussions on the reactor design and directly contributed to the apparatus construction; Robert H. Hauge designed the apparatus and contributed to experimental discussions; W. Wade Adams contributed towards the construction of the apparatus and in discussions about the experiments and results; Andrew R. Barron was involved in the simplification of the apparatus, providing guidance to experiments. All the authors contributed to writing the manuscript.

**Conflicts of Interest:** The authors declare no conflict of interest.

#### References

1. Barron, A.R.; Khan, M.R. Carbon nanomaterials: Opportunities and challenges. *Adv. Mater. Process.* **2008**, *166*, 41–43.
2. O'Connell, M.J.; Bachilo, S.M.; Huffman, C.B.; Moore, V.C.; Strano, M.S.; Haroz, E.H.; Rialon, K.L.; Boul, P.J.; Noon, W.H.; Kittrell, C.; et al. Band gap fluorescence from individual single-walled carbon nanotubes. *Science* **2002**, *297*, 593–596. [[CrossRef](#)]
3. Chen, J.; Hamon, M.A.; Hu, H.; Chen, Y.; Rao, A.M.; Eklund, P.C.; Haddon, R.C. Solution properties of single-walled carbon nanotubes. *Science* **1998**, *282*, 95–98. [[CrossRef](#)]
4. Hamilton, C.E.; Barron, A.R. Phosphene functionalized single walled carbon nanotubes. *Main Group Chem.* **2009**, *8*, 275–281. [[CrossRef](#)]
5. Sun, Y.-P.; Fu, K.; Lin, Y.; Huang, W. Functionalized carbon nanotubes: Properties and applications. *Acc. Chem. Res.* **2002**, *35*, 1096–1104. [[CrossRef](#)]



6. Zeng, L.; Zhang, L.; Barron, A.R. Tailoring aqueous solubility of functionalized single-wall carbon nanotubes over a wide pH range through substituent chain length. *Nano Lett.* **2005**, *5*, 2001–2004. [[CrossRef](#)]
7. Peng, H.; Reverdy, P.; Khabashesku, V.N.; Margrave, J.L. Sidewall functionalization of single-walled carbon nanotubes with organic peroxides. *Chem. Commun.* **2003**, *7*, 362–363. [[CrossRef](#)]
8. Zhang, X.; Sreekumar, T.V.; Liu, T.; Kumar, S. Properties and structure of nitric acid oxidized single wall carbon nanotube films. *J. Phys. Chem. B* **2004**, *108*, 16435–16440. [[CrossRef](#)]
9. Bhakta, A.K.; Detriche, S.; Martis, P.; Mascarenhas, R.J.; Delhalle, J.; Mekhalif, Z. Decoration of tricarboxylic and monocarboxylic aryl diazonium functionalized multi-wall carbon nanotubes with iron nanoparticles. *J. Mater. Sci.* **2017**. [[CrossRef](#)]
10. Holzinger, M.; Vostrowsky, O.; Hirsch, A.; Hennrich, F.; Kappes, M.; Weiss, R.; Jellen, F. Sidewall functionalization of carbon nanotubes. *Angew. Chem. Int. Ed.* **2001**, *40*, 4002–4005. [[CrossRef](#)]
11. Boul, P.J.; Liu, J.; Mickelson, E.T.; Huffman, C.B.; Ericson, L.M.; Chiang, I.W.; Smith, K.A.; Colbert, D.T.; Hauge, R.H.; Margrave, J.L.; et al. Reversible sidewall functionalization of buckytubes. *Chem. Phys. Lett.* **1999**, *310*, 367–372. [[CrossRef](#)]
12. Dillon, E.P.; Andreoli, E.; Cullum, L.; Barron, A.R. Polyethyleneimine functionalized nanocarbons for the efficient absorption of carbon dioxide with a low temperature of regeneration. *J. Exp. Nanosci.* **2015**, *10*, 746–768. [[CrossRef](#)]
13. Zhang, L.; Yang, J.; Edwards, C.L.; Alemany, L.B.; Khabashesku, V.N.; Barron, A.R. Diels alder addition to fluorinated single walled carbon nanotubes. *Chem. Commun.* **2005**, *14*, 3265–3267. [[CrossRef](#)]
14. Liang, F.; Sadana, A.K.; Peera, A.; Chattopadhyay, J.; Gu, Z.; Hauge, R.H.; Billups, W.E. A convenient route to functionalized carbon nanotubes. *Nano Lett.* **2004**, *4*, 1257–1260. [[CrossRef](#)]
15. Chattopadhyay, J.; Sadana, A.K.; Liang, F.; Beach, J.M.; Xiao, Y.; Hauge, R.H.; Billups, W.E. Carbon nanotube salts. Arylation of single-wall carbon nanotubes. *Org. Lett.* **2005**, *7*, 4067–4069. [[CrossRef](#)]
16. Anderson, R.E.; Barron, A.R. Solubilization of single-wall carbon nanotubes in organic solvents without sidewall functionalization. *J. Nanosci. Nanotechnol.* **2007**, *7*, 3436–3440. [[CrossRef](#)]
17. Birch, A.J. Reduction by dissolving metals. Part I. *J. Chem. Soc.* **1944**, 430–436. [[CrossRef](#)]
18. Wilds, A.L.; Nelson, N.A. A superior method for reducing phenol ethers to dihydro derivatives and unsaturated ketones. *J. Am. Chem. Soc.* **1953**, *75*, 5360–5365. [[CrossRef](#)]
19. Billups, W.E.; Sadana, A.K.; Liang, F.; Hauge, R.H. Reductive Functionalization of Carbon Nanotubes. U.S. Patent 7,758,841, 20 July 2010.
20. Borondics, F.; Bokor, M.; Matus, P.; Tompa, K.; Pekker, S.; Jakab, E. Reductive functionalization of carbon nanotubes. *Fuller. Nanotub. Carbon. Nan.* **2007**, *13*, 375–382. [[CrossRef](#)]
21. Joshi, D.K.; Sutton, J.W.; Carver, S.; Blanchard, J.P. Experiences with commercial production scale operation of dissolving metal reduction using lithium metal and liquid ammonia. *Org. Process Res. Dev.* **2005**, *9*, 997–1002. [[CrossRef](#)]
22. Liang, F.; Alemany, L.B.; Beach, J.M.; Billups, E.W. Structure analyses of dodecylated single-walled carbon nanotubes. *J. Am. Chem. Soc.* **2005**, *127*, 13941–13948. [[CrossRef](#)]
23. Zhang, L.; Zhang, J.; Schmandt, N.; Cratty, J.; Khabashesku, V.N.; Kelly, K.F.; Barron, A.R. AFM and STM characterization of thiol and thiophene functionalized SWNTs: Pitfalls in the use chemical markers to determine the extent of side-wall functionalization in SWNTs. *Chem. Commun.* **2005**, 5429–5430. [[CrossRef](#)]
24. Dresselhaus, M.S.; Pimenta, M.A.; Ecklund, P.C.; Dresselhaus, G. *Raman Scattering in Materials Science*; Webber, W.H., Merlin, R., Eds.; Springer: Berlin, Germany, 2000.
25. Gomez, V.; Irusta, S.; Lawal, O.B.; Adams, W.; Hauge, R.H.; Dunnill, C.W.; Barron, A.R. Enhanced purification of carbon nanotubes by microwave and chlorine cleaning procedures. *RSC Adv.* **2016**, *6*, 11895–11902. [[CrossRef](#)]

